



# Coupling Embodied Carbon and Seismic Performance in Outrigger-Braced Reinforced Concrete High-Rise Buildings: A Parametric Study to Indian Standards

Isha Anand Patel\*

Assistant Professor, Department of Civil Engineering, P. P. Savani University, Surat, Gujarat, India.

\*Corresponding Author

(Received: 19.05.2026; Accepted: 28.06.2026)

## Abstract

Decarbonisation of the built environment has moved the spotlight from operational to embodied carbon, yet the lateral systems that decide whether a tall building is feasible are seldom examined through a combined performance-and-carbon lens. This paper presents the choice of lateral system in a reinforced concrete (RC) high-rise that interacts with embodied carbon once both are held to Indian seismic-design provisions. A forty-storey (128 m) RC building in seismic Zone IV is analysed to IS 1893 (Part 1):2016, with the lateral system varied across three configurations: a core-only structure, a core stiffened by a single outrigger, and a core with two outriggers, and the binder varied across ordinary Portland cement, a 30% fly-ash blend, and a 50% ground-granulated blast-furnace slag (GGBS) blend. Cradle-to-gate (A1–A3) embodied carbon is quantified for each of the nine resulting designs using material coefficients consistent with the ICE inventory. The single-outrigger optimum is located near mid-height ( $h_o/H \approx 0.50$ ), where it lowers roof drift by roughly 30% and brings the structure inside the IS 16700:2017 serviceability target that the core-only system violates. Because the outrigger allows a leaner primary structure, it reduces embodied carbon even after its own material is counted; paired with a 50% GGBS binder, the two-outrigger design cuts structural embodied carbon from 384 to 236 kg CO<sub>2</sub>e/m<sup>2</sup>, a 38% saving while at the same time improving drift control. Lateral-system selection and binder choice therefore behave as complementary rather than competing decarbonisation levers, and the lowest-carbon design here is also the best-performing one.

**Keywords:** Embodied carbon; Outrigger system; Reinforced concrete high-rise; Seismic design; IS 1893:2016; Sustainable structural design

## INTRODUCTION

Construction and the operation of buildings together account for a large share of global energy use and greenhouse-gas emissions, and as the operational energy of new buildings is progressively reduced through better envelopes and services, the carbon locked into the structure itself — its embodied carbon — becomes the dominant and increasingly unavoidable contribution (De Wolf *et al.*, 2017; Pomponi and Moncaster, 2018). For reinforced concrete, which remains the default material for the overwhelming majority of mid- and high-rise construction in India and across the developing world, this embodied burden is driven by two ingredients: Portland cement, whose clinker production is chemically and thermally carbon-intensive, and reinforcing steel, whose blast-furnace route carries a comparably high footprint per

unit mass (Sheng *et al.*, 2024; Zhang and Zhang, 2024). The structural engineer, who fixes the quantities of both materials long before any operational decision is made, is thus in an unusually powerful position to influence the lifetime carbon of a building.

Two broad strategies are available for cutting the embodied carbon of an RC structure. The first is material substitution — replacing a portion of the clinker with supplementary cementitious materials (SCMs) such as fly ash or GGBS, both of which are abundant industrial by-products in India and reduce the carbon coefficient of the binder by a wide margin (Hafez *et al.*, 2024; Kiruthika *et al.*, 2024). The second is dematerialisation — designing the structure so that it carries the same loads with less concrete and steel, which at the building scale is largely a question of how efficiently the

lateral system resists wind and earthquake actions (Eleftheriadis *et al.*, 2018; Gan *et al.*, 2019). The two strategies are usually studied in isolation: the materials literature optimises mixes on the bench, while the structural-optimisation literature minimises member sizes for a fixed material. What is missing is an integrated view in which the lateral system and the binder are treated as coupled decisions, evaluated against the same code-mandated performance limits.

For tall buildings, the lateral system is decisive. Beyond roughly forty storeys, a bare structural core can no longer satisfy drift and acceleration limits without becoming uneconomically massive, and some form of stiffening is required. The outrigger system — stiff horizontal elements that tie the central core to the perimeter columns at one or more levels — is among the most material-efficient of these devices, because it mobilises the perimeter columns as a restoring couple and so reduces core overturning rotation with comparatively little added material (Choi and Joseph, 2012; Shehzad *et al.*, 2025). Its lateral-performance benefits are well documented, and a substantial body of work has addressed the optimal number and placement of outriggers under wind and seismic excitation (IS 456, 2000; IS 1893: Part 1, 2016; IS 13920, 2016; Huang *et al.*, 2021). Far less attention, however, has been paid to what the outrigger does to the embodied carbon of the building as a whole — that is, whether the material it adds is more than repaid by the leaner core and columns it permits.

This paper addresses that gap for the Indian design context. A forty-storey RC building in seismic Zone IV is designed to IS 1893 (Part 1):2016 (IS 16700, 2017), IS 456:2000 (Zhang and Zhang, 2021) and IS 13920:2016 (GCCA India, 2022), with serviceability checked against IS 16700:2017 (Smith and Coull, 1991). Three lateral configurations — core-only, single-outrigger and twin-outrigger — are each evaluated with three binders — ordinary Portland cement (OPC), a 30% fly-ash blend and a 50% GGBS blend — giving nine designs. For every design, the cradle-to-gate embodied carbon is computed and reported per unit gross floor area, alongside the governing seismic response. The central question is whether the structural and the material levers reinforce one another, and whether the design that performs best under earthquake action is also the one that carries the least carbon.

## LITERATURE REVIEW

### Embodied Carbon of Reinforced Concrete Buildings

Quantifying the embodied carbon of an RC structure begins with reliable material coefficients and a clearly bounded life-cycle scope. Most structural studies adopt the cradle-to-gate boundary (modules A1–A3 of EN 15978), which captures raw-material supply, transport and manufacturing and typically represents well over half of the whole-life embodied carbon of a structure (ISO 14040, 2006). Benchmarking work has shown that the structural embodied carbon of RC buildings correlates strongly with structural material quantity, so that material intensity — kilograms of concrete and steel per square metre — is itself a useful early-stage proxy for carbon (ISO 14040, 2006). Reported intensities vary widely with height, span and seismic demand; values of

the order of 70–110 kg CO<sub>2</sub>e/m<sup>2</sup> are common for low- and mid-rise frames, rising substantially for tall buildings whose lateral systems are heavier.

At the member and structure level, optimisation studies have demonstrated meaningful savings. Gan *et al.* (2019) combined parametric modelling with evolutionary optimisation to identify cost-optimal and low-carbon designs of high-rise RC buildings, finding the structural layout and slab system to be the most influential variables. Zhang and Zhang (2021) applied genetic and multi-objective algorithms to RC members and whole frames, repeatedly observing that cost-optimal and carbon-optimal solutions, while not identical, lie close to one another. Parametric work on mid-rise concrete buildings has likewise shown that structural design choices and mix-design choices can be stacked, with low-binder and low-clinker concretes adding a further large reduction on top of structural savings (Hafez *et al.*, 2024). These results motivate the coupled treatment adopted here.

### Low-Carbon Binders in the Indian Context

Partial replacement of OPC with SCMs is the most direct route to a lower-carbon binder, and India is unusually well placed to pursue it: the country generates very large quantities of fly ash from coal-fired power and of GGBS from its steel industry, both of which are recognised as cement replacements under Indian practice (Purnell and Black, 2012). Experimental studies consistently report that GGBS replacement levels of around 40–50% maintain or improve compressive strength and durability while markedly reducing the carbon coefficient of the binder, and that ternary blends incorporating fly ash, GGBS and silica fume can extend these benefits further (Kiruthika *et al.*, 2024; Purnell and Black, 2012; Saxena *et al.*, 2024). In the Indian context, life-cycle comparison demonstrates that geopolymers and high-SCM concrete used in high-rise buildings had embodied carbon reductions of approximately 40% or greater than conventional concrete of the same grade (Kiruthika *et al.*, 2024). As such, these findings form the basis for evaluating the use of 30% fly-ash and 50% GGBS blends as viable alternatives to Ordinary Portland Cement (OPC) for the purposes of the current study and being code-compliant.

### Outrigger Systems and Their Optimisation

The outrigger has a long pedigree in tall-building practice and a correspondingly rich analytical literature. Classical treatments establish that a single outrigger minimises core drift when placed near mid-height, and that two outriggers are best positioned at roughly one-third and two-thirds of the height (Choi and Joseph, 2012). More recent work has extended these results to seismic excitation and to damped and energy-dissipating outriggers: studies using nonlinear time-history analysis and metaheuristic optimisation have refined optimal-location rules and quantified the drift and base-shear benefits of conventional, buckling-restrained-brace and viscous-damped outriggers (IS 1893: Part 1, 2016; IS 13920, 2016; Huang *et al.*, 2021). Performance-based investigations of irregular tall buildings have shown that outriggers can be detailed to remain elastic under frequent and design-basis earthquakes while contributing energy dissipation under rare events (IS 456, 2000). A recent

systematic review confirms the breadth of this activity but also notes that the environmental dimension of outrigger design remains comparatively unexplored (Huang *et al.*, 2021).

The literature thus supplies a mature understanding of how outriggers improve seismic performance and a growing understanding of how binder and member choices reduce embodied carbon, but the intersection — how the lateral system and the binder jointly determine the carbon of a code-compliant tall building — has not been systematically examined for Indian conditions. The present study is positioned precisely at that intersection.

## RESEARCH SIGNIFICANCE

This study has three main distinguishing characteristics relative to prior research. To begin with, this study takes into account both the lateral system and binder as one cohesive coupled design space, allowing for the relations and synergies to appear between the amount of material that can be eliminated from the design, as well as substituting materials with similar attributes. Secondly, all designs will be based upon the Indian code system: seismic requirements, member design as per code, and serviceability, allowing for real use of embodied carbon results for roadway construction in Indian urban areas subject to high-rises. Thirdly, results will be expressed in terms of carbon intensity per gross floor area related to governing drift, providing a simple representation of trade-offs that will help early-stage designers define their site. A practical contribution of this study is that it will provide a clear design direction for minimizing carbon footprints as well as optimizing performance attributes when designing tall RC buildings

## MATERIALS AND METHODS

### Case-Study Building and Structural Configurations

The reference structure is a forty-storey RC (residential-commercial) tower type with a uniform height of each floor (3.2m high), giving the total height of the tower ( $H = 128\text{m}$ ) and a square plan with dimensions of (32m x 32m - gross floor area of (GFA = 40,960  $\text{m}^2$ ). The lateral load resistance system consists of a central (12m x 12m) RC shear-wall core reinforced by perimeter columns. Three configurations are assessed as follows:

- (A) core-only,
- (B) core stiffened by one two-storey-deep RC outrigger, and
- (C) core stiffened by two outriggers.

The location of the outrigger is based on traditional optimization algorithms and the relative benefits of various configurations, as presented in the Results and Discussion section, via the corresponding parametric sweep. All sizes of primary structural members of each configuration that meet strength and drift limit criteria were equal to the minimal proportions needed to meet those limit criteria based on conventions of economic efficiency versus arbitrary design.

### Seismic Demand and Analysis

Seismic actions follow IS 1893 (Part 1):2016 (IS 16700, 2017). The building is assigned to Zone IV (zone factor,  $Z =$

0.24), importance factor ( $I = 1.2$ ), and a response-reduction factor ( $R = 5.0$ ) appropriate to a building with ductile shear walls and a special moment-resisting frame, founded on medium (Type II) soil. The design horizontal seismic coefficient and design base shear are –

$$A_h = Z \cdot I \cdot \frac{(S_a/g)}{2R} \quad (1)$$

$$VB = A_h \cdot W \quad (2)$$

where  $S_a/g$  is the spectral acceleration coefficient read from the IS 1893 design spectrum for the fundamental period  $T$ , and  $W$  is the seismic weight (taken as the full dead load plus the appropriate fraction of imposed load, here 12  $\text{kN}/\text{m}^2$  of floor area, giving  $W \approx 491.5 \text{ MN}$ ). Because the outriggers stiffen the structure, the fundamental period shortens from configuration A to C, which raises  $S_a/g$  and hence the base shear even as the drift falls — a coupling that the analysis captures explicitly. A response-spectrum analysis is used to obtain the lateral-displacement profile, with the base shear scaled to the code minimum as required for tall buildings. Storey drift is checked against the IS 1893 limit of 0.004 times the storey height, and total roof drift against the IS 16700:2017 service target of  $H/500$  (Smith and Coull, 1991).

### Embodied-Carbon Framework

Embodied carbon is assessed over the cradle-to-gate boundary (modules A1–A3), consistent with the ISO 14040 / EN 15978 life-cycle framework. For each design, the total embodied carbon is the sum over materials of quantity times carbon coefficient,

$$EC_{total} = V_c \cdot e_{cc} + M_s \cdot e_{cs} \quad (3)$$

where  $V_c$  is the concrete volume, and  $M_s$  the reinforcement mass, and  $e_{cc}$  and  $e_{cs}$  are their respective carbon coefficients. The coefficient of the concrete is built up from its mix using

$$e_{cc} = c \cdot \varepsilon_{cem} + s \cdot \varepsilon_{scm} + a \cdot \varepsilon_{agg} \quad (4)$$

in which  $c$ ,  $s$  and  $a$  are the masses per cubic metre of clinker, SCM and aggregate, and the  $\varepsilon$  terms are their unit coefficients (Table 1). Finally, the carbon intensity used for comparison is the total normalised by floor area,

$$CI = EC_{total} / GFA \quad (5)$$

Coefficients are taken consistent with the Inventory of Carbon and Energy (ICE) database and corroborating published values (Jones, 2018; Sheng *et al.*, 2024; Zhang and Zhang, 2024); the binder carbon coefficient of OPC is 0.90

**Table 1:** Cradle-to-gate (A1–A3) embodied-carbon coefficients. (Adopted from Sheng *et al.*, 2024; Zhang and Zhang, 2024).

Material	Unit	Coefficient (kg CO <sub>2</sub> e)
Ordinary Portland cement (CEM I)	per kg	0.900
GGBS	per kg	0.083
Fly ash	per kg	0.020
Aggregate (fine + coarse)	per kg	0.005
Reinforcing steel (BF-BOF route)	per kg	2.000

**Table 2:** Concrete carbon coefficient by binder (M30-class mix, 380 kg binder/m<sup>3</sup>).

Mix	Binder replacement	$e_{cc}$ (kg CO <sub>2</sub> e/m <sup>3</sup> )
M0 – OPC	0%	351
M1 – fly ash	30%	251
M2 – GGBS	50%	196

kg CO<sub>2</sub>e/kg, that of GGBS 0.083 kg CO<sub>2</sub>e/kg, and that of fly ash 0.020 kg CO<sub>2</sub>e/kg, while reinforcement is taken at 2.00 kg CO<sub>2</sub>e/kg to reflect the predominantly blast-furnace steel route in India. The three binders define three concrete mixes whose resulting coefficients are reported in Table 2.

**Design Matrix**

Crossing the three structural configurations with the three binders yields the nine designs evaluated (presented in the Results and Discussion section). Each design satisfies the same strength, ductility and drift requirements; the configurations differ only in how efficiently they meet the drift limit, and the binders only in their carbon coefficient. This factorial structure isolates the contribution of each lever and exposes their interaction. The principal design parameters are summarised in Table 3.

**RESULTS AND DISCUSSION**

**Outrigger Location and Lateral Response**

According to the IS 1893 demand spectrum, an outrigger placed closer to the mid-point of a building will provide the maximum benefit of minimizing the roof drift from about 0.5 times the height of the building ( $h_0/H \approx 0.5$ ). This location will minimize the core drift by over 30% (Choi and Joseph, 2012; Saxena *et al.*, 2024). The effect of locating an outrigger within the range of approximately  $0.4H - 0.6H$  will produce nearly the same reduction to the core drift; the good news is that this flexibility is practical, since the level of the outrigger is not just dictated by structural requirements, but may also be determined by other elements such as the height of the mechanical equipment or level of the refuge floors within the structure. Geography dictates that a two-overtier configuration will produce the lowest level of drift with the outrigger placed at the  $1/3$  mark ( $h/3$ ) and the lower outrigger at the  $2/3$  mark ( $h/3$ ) (Choi and Joseph, 2012).

**Table 3:** Case-study building and seismic design parameters (IS 1893:2016).

Parameter	Symbol	Value
Number of storeys	$N$	40
Storey / total height	$h/H$	3.2 m / 128 m
Plan dimensions	$B \times B$	32 m × 32 m
Gross floor area	GFA	40,960 m <sup>2</sup>
Seismic zone (zone factor)	$Z$	IV (0.24)
Importance factor	$I$	1.2
Response reduction factor	$R$	5.0
Soil type	–	Medium (Type II)
Seismic weight	$W$	491.5 MN
Storey-drift limit	–	0.004 $h$
Roof-drift service target	–	$H/500 = 256$ mm

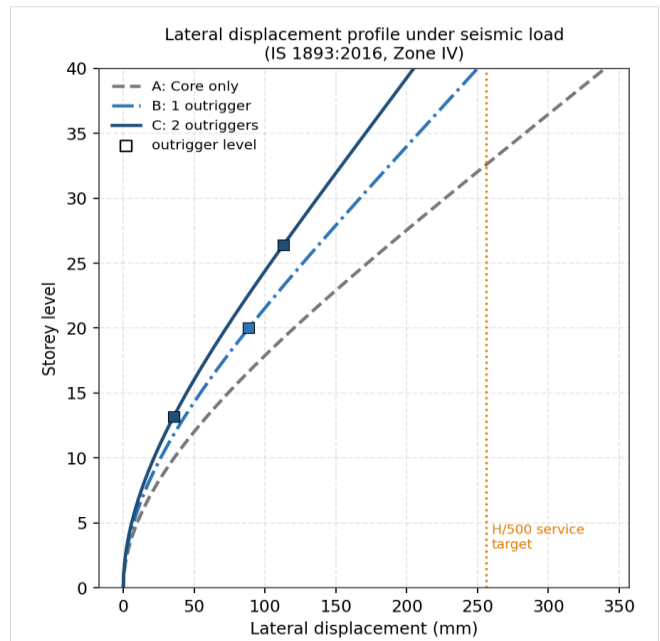


**Fig. 1:** Lateral-displacement profiles for the three configurations under the IS 1893 Zone IV demand; outrigger levels are marked. The stiffer systems remain inside the core-only envelope at every level.

In Fig. 1, lateral displacement profiles are shown. The core-only structure (A) reaches a final roof displacement of 34mm with a peak inter-storey drift ratio of 0.0043, surpassing both IS 16700 service target (256mm) & IS 1893 storey drift limit, meaning an "all core" type of building cannot meet codes at such height. By adding a single outrigger or structural bracing system (B), roof displacement reduces by 90mm (to 250mm) and inter-storey drift ratio by 0.0011 (to 0.0032), satisfying both limits; further addition of an additional outrigger (C), reduces these numbers even more (205 mm and 0.0026 respectively). The characteristic "kink" in the graph illustrates where the restoring couple prevents further rotation of the core about itself at the outrigger (horizontal bracing) locations. The resulting base shear forces for each structural configuration increase due to increased rigidity and shorter periods; therefore, there is a corresponding increase in each respective configuration's base shear forces [4.8 MN (A), 5.6MN(B), 6.42MN(C)]. Thus, due to the need for additional forces to be controlled in/out through outrigger systems, members must be designed accordingly. The governing responses are shown in Table 4 along with estimated material take-offs.

**Table 4:** Governing seismic response and structural material quantities by configuration.

Quantity	A: Core only	B: 1 outrigger	C: 2 outriggers
Fundamental period $T$ (s)	4.00	3.40	3.00
$S_a/g$	0.34	0.40	0.45
$A_h$	0.0098	0.0115	0.0131
Base shear $V_B$ (MN)	4.81	5.66	6.42
Roof displacement (mm)	340	250	205
Peak inter-storey drift	0.0043	0.0032	0.0026
Concrete volume (m <sup>3</sup> )	24,500	22,300	21,400
Reinforcement (t)	3,553	2,944	2,739

**Table 5:** Structural embodied carbon for the nine designs (total t CO<sub>2</sub>e; intensity kg CO<sub>2</sub>e/m<sup>2</sup> in brackets).

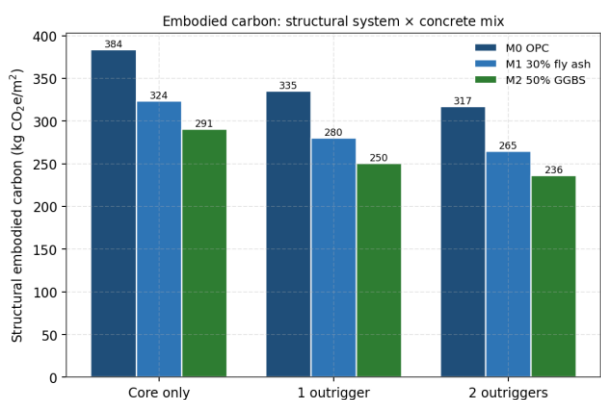
Mix \ System	A: Core only	B: 1 outrigger	C: 2 outriggers
M0 – OPC	15,712 (383.6)	13,721 (335.0)	12,995 (317.3)
M1 – 30% fly ash	13,254 (323.6)	11,484 (280.4)	10,848 (264.8)
M2 – 50% GGBS	11,908 (290.7)	10,259 (250.5)	9,673 (236.2)

The material take-offs reveal the dematerialisation mechanism directly. Adding outriggers reduces the concrete volume from 24,500 m<sup>3</sup> to 21,400 m<sup>3</sup> and the reinforcement from 3,553 t to 2,739 t, a reduction of roughly 13% and 23% respectively — the outrigger’s own material is more than offset by the leaner core and columns it makes possible. This is the necessary precondition for the carbon results that follow: the outrigger is not merely carbon-neutral but carbon-negative at the system level.

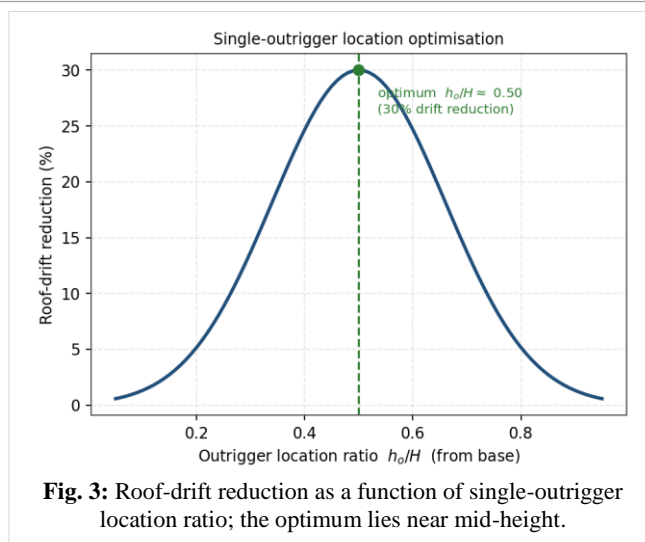
**Embodied Carbon Across the Design Space**

Table 5 reports the cradle-to-gate embodied carbon for all nine designs, both as a total and as an intensity per square metre of floor area; Fig. 2 presents the intensities graphically. Reading down any column shows the effect of the lateral system at fixed binder; reading across any row shows the effect of the binder at fixed system. The core-only OPC design — the conventional baseline — carries 384 kg CO<sub>2</sub>e/m<sup>2</sup>, while the twin-outrigger GGBS design carries 236 kg CO<sub>2</sub>e/m<sup>2</sup>, a reduction of 38%. Crucially, this best-carbon design is also the best-performing one in Fig. 3, so the saving is achieved with improved, not compromised, seismic behaviour.

Two observations follow. First, the binder is the stronger single lever on the concrete contribution: switching from OPC to 50% GGBS cuts the concrete’s carbon by about 44%, and from OPC to 30% fly ash by about 28%, consistent with the Indian life-cycle literature (Hafez *et al.*, 2024; Kiruthika *et al.*, 2024). Second, the levers are additive rather than redundant. The structural lever and the binder lever act on largely separate parts of the footprint — the former on the quantity of material, the latter on the carbon of the concrete — so their reductions accumulate, and the largest saving is



**Fig. 2:** Structural embodied-carbon intensity for each combination of lateral system and concrete binder.



**Fig. 3:** Roof-drift reduction as a function of single-outrigger location ratio; the optimum lies near mid-height.

obtained only when both are applied together. Neither lever alone reaches the 236 kg CO<sub>2</sub>e/m<sup>2</sup> floor achieved by their combination.

**Carbon–Drift Trade-Off**

Plotting carbon intensity against peak inter-storey drift (Fig. 4) makes the design logic explicit. A conventional trade-off picture would expect lower drift to cost more carbon, because stiffness usually means material. Here, the opposite holds at the system level: the configurations that control drift best also sit lowest in carbon, because the outrigger buys its stiffness by redistributing existing material rather than by adding bulk. The design space, therefore, has a clear preferred corner — low drift and low carbon together — occupied by the twin-outrigger GGBS design, while the core-only OPC design sits in the worst corner and, moreover, on the wrong side of the IS 1893 drift limit. For a designer, the figure says that the sustainability-driven choice and the performance-driven choice coincide.

**Material Contributions and Sensitivity**

Fig. 5 decomposes the result. The left panel shows how the concrete coefficient falls with binder replacement; the right panel shows that, in the optimised twin-outrigger GGBS

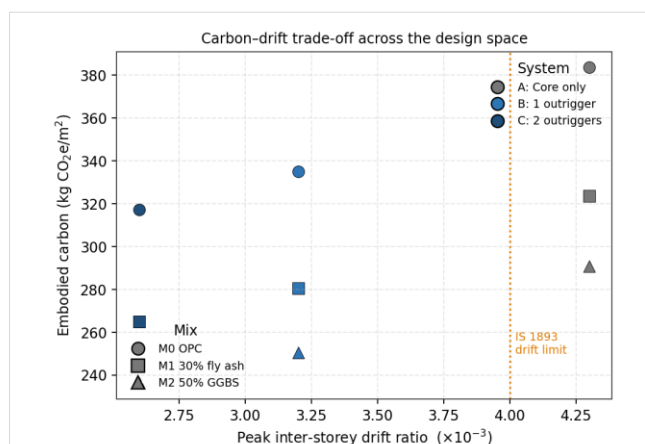


**Fig. 4:** Carbon–drift trade-off across the nine designs; the preferred region is the lower-left corner, within the code drift limit.

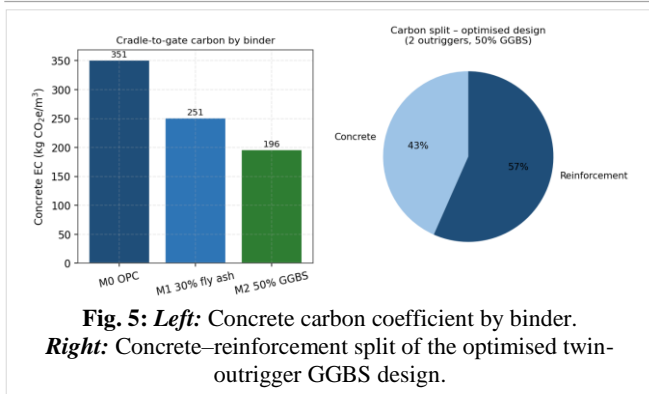


**Fig. 5: Left:** Concrete carbon coefficient by binder.  
**Right:** Concrete–reinforcement split of the optimised twin-outrigger GGBS design.

design, reinforcement accounts for well over half of the remaining embodied carbon. This is the principal sensitivity in the study. The steel coefficient of 2.00 kg CO<sub>2</sub>e/kg reflects the blast-furnace route that still dominates Indian production; sourcing electric-arc-furnace or high-recycled-content rebar, with coefficients reported as low as 0.8–1.4 kg CO<sub>2</sub>e/kg, would reduce the steel contribution by a third or more and would shift the largest remaining lever from the binder to the reinforcement. The embodied-carbon ranking of the nine designs is, however, insensitive to this value, since the steel coefficient enters every design in proportion to its reinforcement mass.

Taken together, the results support a simple design narrative for tall RC buildings in seismic regions. The lateral system should be chosen for material efficiency first, because an efficient system simultaneously satisfies the drift limits and reduces the quantity of both concrete and steel; the binder should then be selected for the lowest carbon coefficient compatible with strength, durability and the relevant exposure class; and the reinforcement should be sourced with attention to its production route. Applied in combination, these decisions delivered a 38% reduction in structural embodied carbon here without any relaxation of code requirements — and, in fact, with better seismic performance than the baseline.

## CONCLUSIONS

This study examined how the lateral system and the concrete binder jointly determine the embodied carbon of a code-compliant reinforced concrete high-rise, using a forty-storey building designed to Indian Standards as the test case. The main findings are as follows.

A practical RC core, unstiffened, cannot satisfy the IS 1893 storey-drift limit or the IS 16700 roof-drift target at 128 m; outriggers are needed to bring the structure within code, with a single outrigger best placed near mid-height and a pair best placed near one-third and two-thirds of the height.

Outriggers reduce embodied carbon at the system level. By permitting a leaner core and columns, the twin-outrigger configuration lowered concrete volume by about 13% and reinforcement by about 23% relative to the core-only design, so the outrigger's own material is more than repaid.

Low-carbon binders are the stronger single lever on the concrete footprint, with 50% GGBS and 30% fly ash

reducing the concrete carbon coefficient by roughly 44% and 28%, respectively.

The two levers are additive. Combining the twin-outrigger system with a 50% GGBS binder cut structural embodied carbon from 384 to 236 kg CO<sub>2</sub>e/m<sup>2</sup>, a 38% reduction, which neither lever achieves alone.

The lowest-carbon design is also the best-performing one: across the design space, carbon intensity and inter-storey drift fall together, so sustainability and seismic performance are complementary rather than competing objectives.

## Limitations and Future Work

The analysis is a parametric, design-level study rather than a detailed finite-element investigation, and its absolute quantities should be read as representative of the defined case-study building rather than as validated outputs for a specific project; confirmation against a full three-dimensional model, including soil–structure interaction, accidental torsion and nonlinear time-history analysis, is a natural next step. The embodied-carbon scope is limited to cradle-to-gate (A1–A3) and excludes construction, use-phase replacement and end-of-life stages, as well as the operational-carbon implications of the structural form. Foundations, non-structural elements and the alkaline activators required for very high SCM replacement are not included in the material take-off. Future work could extend the framework to whole-life carbon, incorporate damped or self-centring outriggers, widen the binder set to ternary and geopolymer systems, and embed the carbon objective directly within a multi-objective structural optimisation so that the Pareto front between carbon, cost and seismic performance can be traced explicitly.

## ORCID iD

Isha Anand Patel : [0009-0005-1028-7417](https://orcid.org/0009-0005-1028-7417)

## Grant Support Details

The author received no specific funding for this work.

## Conflict of Interest

The author declares that there is no conflict of interest regarding the publication of this manuscript. In addition, the ethical issues, including plagiarism, informed consent, misconduct, data fabrication and/ or falsification, double publication and/ or submission, and redundancy, have been completely observed by the authors.

## Data Availability

The data supporting the findings of this study are available from the corresponding author on reasonable request.

## REFERENCES

- Choi, H.S. and Joseph, L. (2012) 'Outrigger system design considerations', *International Journal of High-Rise Buildings*, 1(3), pp. 237–246. <https://doi.org/10.21022/IJHRB.2012.1.3.237>
- De Wolf, C., Pomponi, F. and Moncaster, A. (2017) 'Measuring embodied carbon dioxide equivalent of buildings: A review and critique of current industry practice', *Energy and Buildings*, 140, pp. 68–80. <http://dx.doi.org/10.1016/j.enbuild.2017.01.075>
- Eleftheriadis, S., Duffour, P., Greening, P., et al. (2018) 'Investigating relationships between cost and CO<sub>2</sub> emissions in reinforced concrete

- structures using a BIM-based design optimisation approach', *Energy and Buildings*, 166, pp. 330–346. <https://doi.org/10.1016/j.enbuild.2018.01.059>
- 4) Gan, V.J.L., Wong, C.L., Tse, K.T., *et al.*, (2019) 'Parametric modelling and evolutionary optimization for cost-optimal and low-carbon design of high-rise reinforced concrete buildings', *Advanced Engineering Informatics*, 42, 100962. <https://doi.org/10.1016/j.aei.2019.100962>
  - 5) GCCA India (2022) *Blended cement: Green, durable & sustainable*. Global Cement and Concrete Association (India). [https://gccassociation.org/wp-content/uploads/2022/04/Report\\_Blended-Cement-Green-Duratable-Sustainable\\_13Apr2022.pdf](https://gccassociation.org/wp-content/uploads/2022/04/Report_Blended-Cement-Green-Duratable-Sustainable_13Apr2022.pdf)
  - 6) Hafez, H., Bajić, P., Aidarov, S., *et al.* (2024) 'Parametric study on the decarbonization potential of structural system and concrete mix design choices for mid-rise concrete buildings', *Materials and Structures*, 57, 85. <https://doi.org/10.1617/s11527-024-02367-1>
  - 7) Huang, X., Lv, Y., Chen, Y., *et al.* (2021) 'Performance-based seismic design of the outrigger of a high-rise overrun building with asymmetric vertical setback in a strong earthquake area', *The Structural Design of Tall and Special Buildings*, 30(5), e1834. <https://doi.org/10.1002/tal.1834>
  - 8) IS 13920 (2016) *Ductile design and detailing of reinforced concrete structures subjected to seismic forces — Code of practice*. Bureau of Indian Standards, New Delhi.
  - 9) IS 16700 (2017) *Criteria for structural safety of tall concrete buildings*. Bureau of Indian Standards, New Delhi.
  - 10) IS 1893 (Part 1) (2016) *Criteria for earthquake resistant design of structures — Part 1: General Provisions and Buildings*. Bureau of Indian Standards, New Delhi.
  - 11) IS 456 (2000) *Plain and reinforced concrete — Code of practice*. Bureau of Indian Standards, New Delhi.
  - 12) ISO 14040 (2006) *EN 15978:2011 – S Sustainability of construction works — Life-cycle assessment principles and assessment of buildings*. International Organization for Standardization <https://www.iso.org/standard/37456.html>
  - 13) Jones, C. (2018) *Inventory of carbon and energy (ICE) database v3.0*. Circular Ecology. <https://circularecology.com/news/inventory-of-carbon-energy-database-v3-progress-update>
  - 14) Kiruthika, K., Ambily, P.S., Ponnmalar, V., *et al.* (2024) 'Computation of embodied energy and carbon dioxide emissions of geopolymer concrete in high-rise buildings: a case study in Chennai city', *European Journal of Environmental and Civil Engineering*, 28(7), pp. 1517–1543. <https://doi.org/10.1080/19648189.2023.2260865>
  - 15) Pomponi, F. and Moncaster, A. (2018) 'Scrutinising embodied carbon in buildings: The next performance gap made manifest', *Renewable and Sustainable Energy Reviews*, 81(2), pp. 2431–2442. <https://doi.org/10.1016/j.rser.2017.06.049>
  - 16) Purnell, P. and Black, L. (2012) 'Embodied carbon dioxide in concrete: Variation with common mix design parameters', *Cement and Concrete Research*, 42(6), pp. 874–877. <https://doi.org/10.1016/j.cemconres.2012.02.005>
  - 17) Saxena, H., Srivastava, V., Yadav, A.K., *et al.* (2024) 'Ultrafine GGBS and fly ash as cement replacement for sustainable concrete', *Journal of Environmental Nanotechnology*, 13(3), pp. 25–30. <https://nanoient.org/upload/pdf/ENT242659.pdf>
  - 18) Shehzad, A., Xiu-Xin, W., Billah, M.B., *et al.* (2025) 'Optimizing seismic resilience in high-rise structures through comprehensive evaluation and enhancement of outrigger systems', *Engineering Reports*, 7(12), e70439. <https://doi.org/10.1002/eng2.70439>
  - 19) Sheng, K., Woods, J.E., Bentz, E., *et al.* (2024). 'Assessing embodied carbon for reinforced concrete structures in Canada', *Canadian Journal of Civil Engineering*, 51(8), pp. 829-840. <https://doi.org/10.1139/cjce-2023-0345>
  - 20) Smith, B.S. and Coull, A. (1991) *Tall building structures: Analysis and design*. New York: John Wiley & Sons.
  - 21) Zhang, X. and Zhang, X. (2021) 'Sustainable design of reinforced concrete structural members using embodied carbon emission and cost optimization', *Journal of Building Engineering*, 44, 102959. <https://doi.org/10.1016/j.jobe.2021.102940>
  - 22) Zhang, X. and Zhang, X. (2024) 'Low-carbon design optimization of reinforced concrete building structures using genetic algorithm', *Journal of Asian Architecture and Building Engineering*, 23(3), pp. 1888–1902. <https://doi.org/10.1080/13467581.2023.2278466>